

Graphene Crystal Growth Engineering on Epitaxial Copper Thin Films

Robert M. Jacobberger and Michael S. Arnold

Department of Materials Science and Engineering, University of Wisconsin-Madison, Madison, Wisconsin, United States
jacobberger@wisc.edu

In this work¹, we study graphene growth dynamics on epitaxial Cu thin film substrates by chemical vapor deposition (CVD). These surfaces have a single crystallographic orientation and are atomically smooth, unlike their foil counterparts, making them better platforms on which to reproducibly synthesize high-quality graphene and study crystal growth evolution. Consequently, we gained novel insight into the key mechanisms and factors that influence graphene growth dynamics, such as Mullins-Sekerka morphological instabilities, Cu surface orientation, hydrogen-to-methane flux ratio ($H_2:CH_4$), absolute pressure, and nucleation density. We demonstrate how the various graphene morphologies that are commonly reported in literature, such as lobes, dendrites, hexagrams, and hexagons, can be selectively synthesized over large areas by controlling critical CVD parameters. In particular, growth on Cu(111) can be tuned to yield high-quality, large-scale, single-crystalline graphene monolayers, a feat that is not possible on Cu foil due to the rotational grain boundaries that exist when graphene islands on neighboring Cu facets merge.

Recently, there has been a tremendous effort to control graphene growth dynamics with the goal of tailoring its structure, and therefore, its properties, for specific applications. The extraordinary electronic, thermal, and mechanical properties that graphene possesses are highly dependent on its physical characteristics, including crystallinity, grain size, edge termination, and morphology. While numerous graphene morphologies with various orientations have been synthesized via CVD on polycrystalline Cu foils, the conditions that yield such structures are not well defined and the mechanisms that govern their evolution are not sufficiently understood. This lack of understanding can be attributed to complications in analyzing growth on Cu foils due to their polycrystalline nature and high surface roughness. The numerous foil surface orientations impact growth processes differently due to unique catalytic activity and thermodynamic properties, causing local variations in growth conditions across the substrate. Here, we minimize these local deviations by conducting growth on ultra-smooth, epitaxial Cu(100), Cu(110), and Cu(111) thin films (Figure 1) that have roughness < 1 nm over $10 \times 10 \mu m^2$ areas.

We studied the morphological evolution of graphene crystals in atmospheric pressure CVD (APCVD) and low pressure CVD (LPCVD) with low $H_2:CH_4$ (Figure 2). Initially, the graphene islands are circular (Figure 2a). However, as they exceed a critical size $\sim 1.0 \mu m$, dendritic branches begin to propagate from the crystal perimeter (Figure 2b-h). In LPCVD, the dendrites extend hundreds of microns in the $\langle 100 \rangle$, $\langle 111 \rangle$, and $\langle 110 \rangle$ directions on Cu(100), Cu(110), and Cu(111), respectively; whereas in APCVD, no such relationships exist, resulting in circular dendritic structures. Twin boundaries on the Cu(111) surface disrupt the preferred direction of graphene propagation in LPCVD, making the growth appear more isotropic. Furthermore, we present evidence that the lobed islands commonly grown in LPCVD would evolve into highly dendritic structures if the inter-nucleation spacing was sufficiently large ($\sim 10 \mu m$) (Figure 2i). This observed morphological evolution suggests that graphene growth is driven by Mullins-Sekerka morphological instabilities and is limited by mass transport.

In both pressure regimes, the dendritic nature of growth is suppressed with increasing $H_2:CH_4$, resulting in more compact islands with planar edges. In LPCVD, the dendrite tip angle increases until the branches are entirely "filled in," resulting in squares, rectangles, circles, and hexagons on Cu(100), Cu(110), twinned Cu(111), and non-twinned Cu(111) which reflect the underlying Cu crystal symmetry (Figure 3). Twins disrupt the preferential propagation of graphene in the $\langle 110 \rangle$ direction on Cu(111) (Figure 3i and inset). In APCVD, the islands transition from circular dendritic structures to hexagrams to hexagons with increasing $H_2:CH_4$, regardless of the surface orientation and the presence of twins (Figure 4). The graphene domains have one orientation with respect to the Cu(111) surface, and multiple preferred orientations with respect to the Cu(100) and Cu(110) surfaces. The epitaxial nature of growth on Cu(111) provides a route to manufacture single-crystalline graphene over large scales, eliminating the rotational grain boundaries that degrade charge and heat transport through graphene and that are unavoidable with growth on Cu foils due to their polycrystallinity.

Finally, we show that all growth regimes can result in high-quality continuous monolayer graphene with D:G Raman ratio < 0.1 , demonstrating the utility of this growth technique (Figure 5).

The synthetic method presented here provides a detailed roadmap to tailor the structure, orientation, and morphology of graphene over large areas. The understanding gained from this work will improve crystal growth engineering of graphene and other two-dimensional materials, and will ultimately help lead to the scalable fabrication of defect-free, high-quality graphene materials with superior electrical, thermal, and mechanical properties.

References

[1] Jacobberger, R. M.; Arnold, M. S., *Chem. Mater.*, Submitted.

Figures

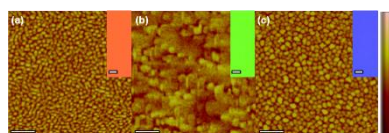


Figure 1. Atomic force microscopy topographical map of Cu films after sputtering. (a) Cu(100), (b) Cu(110), and (c) Cu(111) films have roughness < 1 nm over $10 \times 10 \mu\text{m}^2$ areas, which is > 50 times smoother than Cu foil at the same scale. Scale bars are 400 nm. (a-c) insets are electron backscatter diffraction data with red, green, and blue corresponding to Cu(100), Cu(110), and Cu(111), respectively. Inset scale bars are 50 μm .

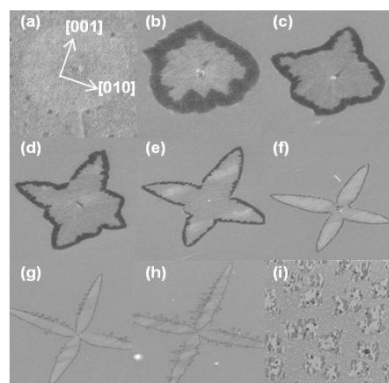


Figure 2. (a-h) Graphene island morphology evolution on Cu(100) in LPCVD with low $\text{H}_2:\text{CH}_4$. Island sizes are (a) 0.7, (b) 1.4, (c) 3.1, (d) 4.9, (e) 7.9, (f) 22, (g) 59, and (h) 115 μm . This evolution suggests that dendritic structures are caused by Mullins-Sekerka instabilities. A similar evolution occurs in APCVD with low $\text{H}_2:\text{CH}_4$, but the figure has been omitted here due to length restrictions. (i) The dendritic nature of growth is suppressed due to small inter-

nucleation distance. The islands in (i) are $\sim 6.0 \mu\text{m}$ in length.

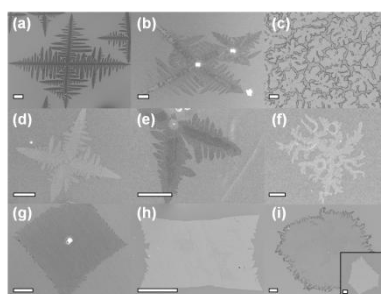


Figure 3. Graphene crystal morphology dependence on $\text{H}_2:\text{CH}_4$ in LPCVD. First, second, and third columns represent the island structure on Cu(100), Cu(110), and twinned Cu(111), respectively. Top, middle, and bottom rows depict island morphology at low, medium, and high $\text{H}_2:\text{CH}_4$, respectively. Scale bars are 40 μm for the first and second columns and 10 μm for the third column. As $\text{H}_2:\text{CH}_4$ is increased, the dendritic nature of growth is suppressed and the graphene islands develop into more planar shapes that reflect the underlying Cu crystallography. (i) inset demonstrates that hexagons form on non-twinned Cu(111) instead of circles.

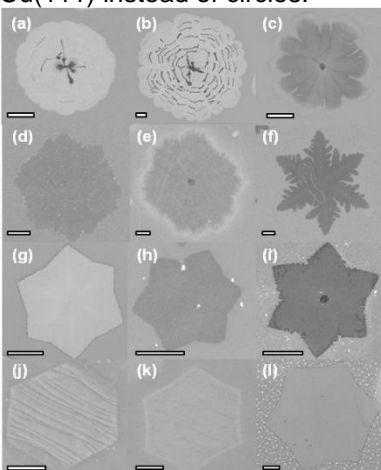


Figure 4. Graphene island morphology dependence on $\text{H}_2:\text{CH}_4$ in APCVD. First, second, and third columns represent the island structure on Cu(100), Cu(110), and Cu(111), respectively. $\text{H}_2:\text{CH}_4$ increases from the top to the bottom row. Scale bars are 5 μm except for 5d and 5j, which are 1 μm . Similar to LPCVD, the dendritic nature of growth is suppressed with increasing $\text{H}_2:\text{CH}_4$. But, in APCVD, the islands evolve into hexagonally-faceted crystals, regardless of the Cu orientation.

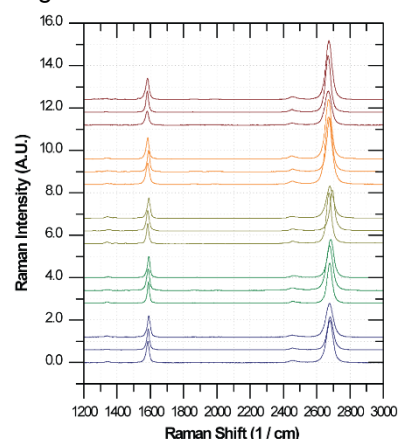


Figure 5. Raman data for continuous, monolayer graphene in all growth regimes. The D:G ratio is < 0.1 , indicating that the graphene is of high-quality. The five sets of spectra, from bottom to top, correspond to dendritic growth in APCVD (blue), hexagram growth in APCVD (green), hexagon growth in APCVD (yellow), dendritic growth in LPCVD (orange), and planar growth in LPCVD (red). The bottom, middle, and top spectra in each color set represent growth on Cu(100), Cu(110), and Cu(111), respectively.